


## TOMOGRAPHIC FINDINGS IN COVID-19 LUNGS: THE CONTRIBUTION OF ARTIFICIAL INTELLIGENCE

 <https://doi.org/10.56238/sevened2025.009-002>

**Bruna Martins Dzivielevski da Camara<sup>1</sup>, Heloisa Severgnini<sup>2</sup>, Georgia Garofani Nasimoto<sup>3</sup>, Rafaella Stradiotto Bernardelli<sup>4</sup>, Auristela Duarte de Lima Moser<sup>5</sup>, Mauren Abreu de Souza<sup>6</sup>**

### ABSTRACT

Since the beginning of the Coronavirus Disease (COVID-19) pandemic, chest CT scans have been a strong ally in the diagnosis and follow-up of patients. New tools have been developed to make lung analysis more objective, such as the 3D Slicer and its Lung Analyser tool. This study aimed to describe the tomographic findings found in patients with COVID-19 admitted to the Care Unit using this tool. **Method.** One hundred and one sets of tomographic images of patients hospitalized between March 2020 and December 2021 with a positive diagnosis of COVID-19 were randomly selected. The Lung Analyser was used to perform the analysis, quantifying the "emphysematous", "infiltrated", "collapsed" and "total affected" lung in milliliters and their percentage. **Findings.** The findings of emphysema remained at around 20% of the volume. Infiltrates, collapsed lungs, and the percentage of total involvement did not show this similarity, with an important plurality of results. In pulmonary infiltrates, the mean involvement rate was 32.98%, with a standard deviation of 0.095. For the percentage of

---

<sup>1</sup> Intensive Care Physician, Master in Health Technology

Pontifical Catholic University of Paraná

brunamd.camara@gmail.com

<https://orcid.org/0000-0002-3166-6679>

<http://lattes.cnpq.br/9034920422196566>

<sup>2</sup> Medical Student

Pontifical Catholic University of Paraná

heloisasevergnini@hotmail.com

<http://lattes.cnpq.br/2249794854889041>

<sup>3</sup> Medical Student

Pontifical Catholic University of Paraná

georgianasimoto@gmail.com

<https://orcid.org/0000-0002-7994-2046>

<http://lattes.cnpq.br/3924070995646608>

<sup>4</sup> Physiotherapist, Master and Doctor in Health Technology

Pontifical Catholic University of Paraná

rafaella.bernardelli@gmail.com

<https://orcid.org/0000-0002-4613-0834>

<http://lattes.cnpq.br/3490380826240683>

<sup>5</sup> Master in Education, PhD in Production Engineering,

Post-Doctorate in Human Functionality and Quality of Life

Pontifical Catholic University of Paraná

auristela.lima@gmail.com

<https://orcid.org/0000-0001-5086-0701>

<http://lattes.cnpq.br/4920711999790713>

<sup>6</sup> Dr. in Medical Physics and Biomedical Engineering,

Master with emphasis in Biomedical Engineering

Pontifical Catholic University of Paraná

mauren.souza@pucpr.br

<https://orcid.org/0000-0001-6137-918X>

<http://lattes.cnpq.br/7932254008088709>

collapsed lung, we have an average of 11.48% and a standard deviation of 0.067. The mean total percentage of lung affected was 44.3%, with a standard deviation of 0.15. **Conclusion:** The description of findings found by the software can be valuable for the identification and quantification of lung lesions in patients with COVID-19, reducing the subjectivity of the reports and helping to better understand lesions, which are sometimes not so visible to the human eye. Its use does not exclude the need for experienced radiologists for the best evaluation.

**Keywords:** 3D Slicer. Lung Analyser. Chest tomography. Covid-19.

## 1 INTRODUCTION

Since the beginning of the COVID-19 pandemic, chest CT has been a strong ally both for initial diagnostic aid and as prognostic staging and follow-up of patients. The most common pattern of involvement on radiological examination is ground-glass predominantly in the periphery of the lungs bilaterally and in bases with areas of greater opacity or attenuation, followed by the simultaneous presence of pulmonary consolidation. New tools have been developed to make the analysis of pulmonary involvement more objective. One of them is 3D Slicer, a free open-source software for medical image computing available for several operating systems (Windows, MAC, Linux) (ABOUT 3DSLICER, [s. d.]) that emerged from the union of several independent projects that focused separately on image visualization, surgical navigation, and graphical user interface (ABOUT 3DSLICER, [s. d.]). Image segmentation followed by the use of the Lung Analyser tool allows the identification of details about the patient's lung involvement, based on levels of Lung Analyser. infiltrate and lung collapse. Such details are not objectively observed by the human eye, thus improving the detailing of lesions automatically with the help of Artificial Intelligence (AI).

The clinical picture of COVID-19 is variable, ranging from mild symptoms, similar to those of flu-like syndrome, such as fever, runny nose, prostration, to pneumonia, severe acute respiratory failure, and death (MENEZES et al., 2021). In clinical practice, it has been observed that the evolution of patients hospitalized for the disease tends to present with a progressive increase in parenchymal lesions, even in those with mild initial involvement (CHANG et al., 2005), with a subsequent decrease in lesions in cases with favorable evolution (ZHOU et al., 2020). We also know that changes in the characterizations of injuries over time can suggest the pattern of progression or recovery of the lesion, being carried out by analyzing the pattern of lesions and the percentage of lung area affected (HANI et al., 2020),(OULEFKI et al., 2020),(COLOMBI et al., 2020). This percentage is usually provided by the radiological report based on a visual and subjective analysis of the images (MARTÍNEZ CHAMORRO et al., 2021), and the involvement is generally divided into mild (< 25% of lung parenchyma affected), moderate (between 25-50% of parenchyma affected) and severe (> 50% of parenchyma affected) or according to the degree of pulmonary aeration in its vast majority (BELL D, MURPHY A, MOREIRA M, [s. d.]),(XIE et al., 2020).

Image segmentation followed by the use of the Lung Analyser tool allows the identification of details about the patient's lung involvement, including the percentage of total volume affected, quantity in volume, and percentage of emphysematous lesions, infiltrate, and lung collapse (PROF. RUDOLF BUMM, DEPARTMENT OF SURGERY, KANTONSSPITAL GRAUBÜNDEN (KSGR), LOESTRASSE 170, CHUR, [n.d.]). Such

information can help in decision-making and in the conduct of health professionals in relation to hospitalized patients (LANZA et al., 2020). With all these aspects demonstrated, we chose to perform a description of the lesions found by 3DSlicer in order to increase knowledge about COVID-19 and assist radiologists in the reports, in order to obtain increasingly accurate and faster reports.

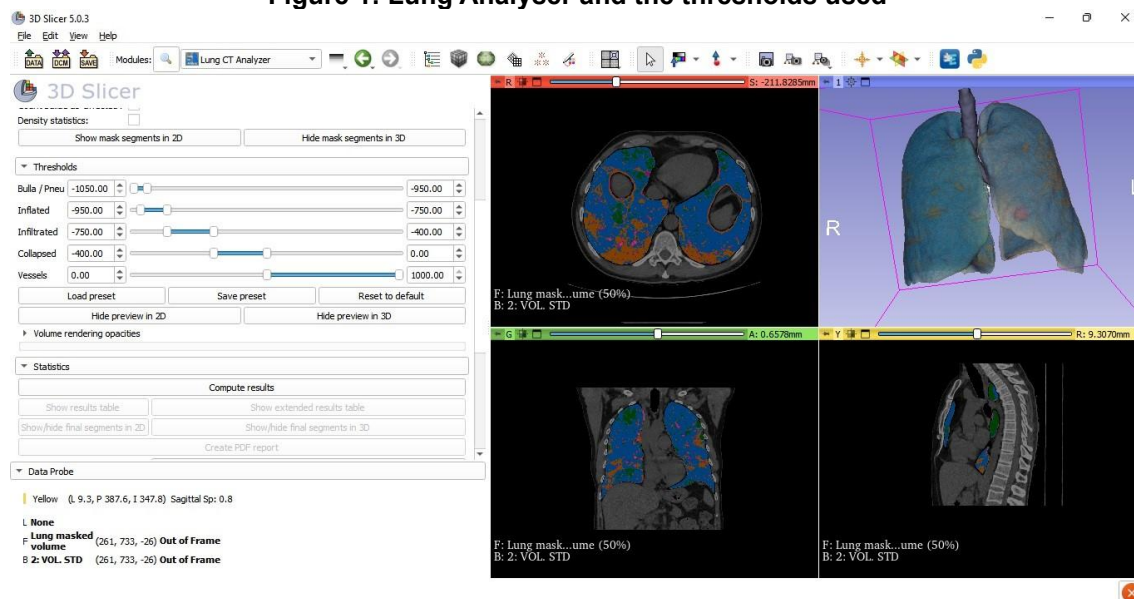
The purpose of this study is to describe the tomographic findings found by the 3D Slicer and its Lung Analyser tool in patients with severe COVID-19 admitted to the Intensive Care Unit (ICU) of a private referral hospital for the treatment of the disease.

## 2 METHODOLOGY

This retrospective study was approved by the local Ethics Committee (opinion 5,347,709). One hundred and one images have been included in this and anonymized to ensure your privacy. The sets were randomly selected from an original pool of patients who had a positive COVID-19 diagnosis by the nasopharyngeal reverse transcription polymerase chain reaction (RT-PCR) swab for SARS-CoV-2 and who underwent a chest CT scan during their ICU stay between March 2020 and December 2021.

The images in DICOM (Digital Image Communication in Medicine) format were imported into 3D Slicer 5.0.3 and the lung masks were automatically segmented by the Lung Segmenter extension using 13 manually tagged dots. Three stitches were placed in axial and coronal sections inside the right and left lungs each, and one stitch in the trachea. The segmentation algorithm uses a grow-cut algorithm with a region of intensity constrained at -3000 to -250 HU (3D SLICER, 2023). All lung masks were visually checked and in some cases (n=6) minor corrections were made manually using "scissors" (cutting a part of the mask) or "fill in slices" (adding a missing part to the lung mask) in the segment editor. The Lung Analyser Extension was then used to perform the analysis of the lung lesions, quantifying the "emphysematous", "infiltrated", "collapsed" and "total affected" lung in milliliters and its percentage in relation to lung volume. Each category mentioned has its own range of HU, namely: emphysematous [-1050; -950HU], infiltrate [-750;-400HU], and collapsed [-400; 0HU] (Figure 1). These limits are variable and the user can modify them manually, however, according to the developers, the limits set by default have already been optimized (3D SLICER COVID-19, 2020) and have therefore been maintained as such in this study.

**Figure 1: Lung Analyser and the thresholds used**



After analysis, the software returns a table with some percentages: particularly, the "Involved" column represents the total amount of the extent of the COVID-19 disease (Figure 2).

By detecting changes in the intensity of UH, the LungAnalyser tool divides pulmonary involvement into collapsed lung, emphysema, infiltrate, and aerated lung, which are important information for the evaluation of pulmonary involvement.

As this study consists of a description of the findings found in the image processing associated with the automatic reading of the 3D Slicer software, more complex statistical calculations were not necessary. To calculate the mean involvement of each lesion, the Excel software was used ( $=\text{MEDIA A2:A102}$ ). To calculate the Standard Deviation, the Excel software was also used by the formula ( $=\text{STDEV A2:A102}$ )

Figure 2 : Example of the file automatically generated after using the Lung Analyser – 3D Slicer tool

### Volumetric analysis (Table 1)

Segment	Volume [cm3]	Minimum [hnsfU]	Maximum [hnsfU]	Mean [hnsfU]	Median [hnsfU]	Standard Deviation [hnsfU]	MinThr	MaxThr
Emphysema right	73.1825	-1024	-951	-995.533	-999	26.3082	-1050	-950
Inflated right	426.475	-950	-751	-838.344	-835	53.79	-950	-750
Infiltration right	342.141	-750	-401	-636.385	-661	90.2909	-750	-400
Collapsed right	68.0295	-400	-1	-234.715	-252	114.029	-400	0
Vessels right	58.7117	-1024	2720	93.8362	85	277.957	0	1000
Emphysema left	52.9877	-1024	-951	-997.022	-1002	26.1595	-1050	-950
Inflated left	229.209	-950	-751	-842.947	-841	54.7014	-950	-750
Infiltration left	170.339	-750	-401	-634.71	-658	90.8528	-750	-400
Collapsed left	37.1256	-400	-1	-231.09	-247	114.709	-400	0
Vessels left	49.1415	-1024	2420	61.967	71	230.689	0	1000

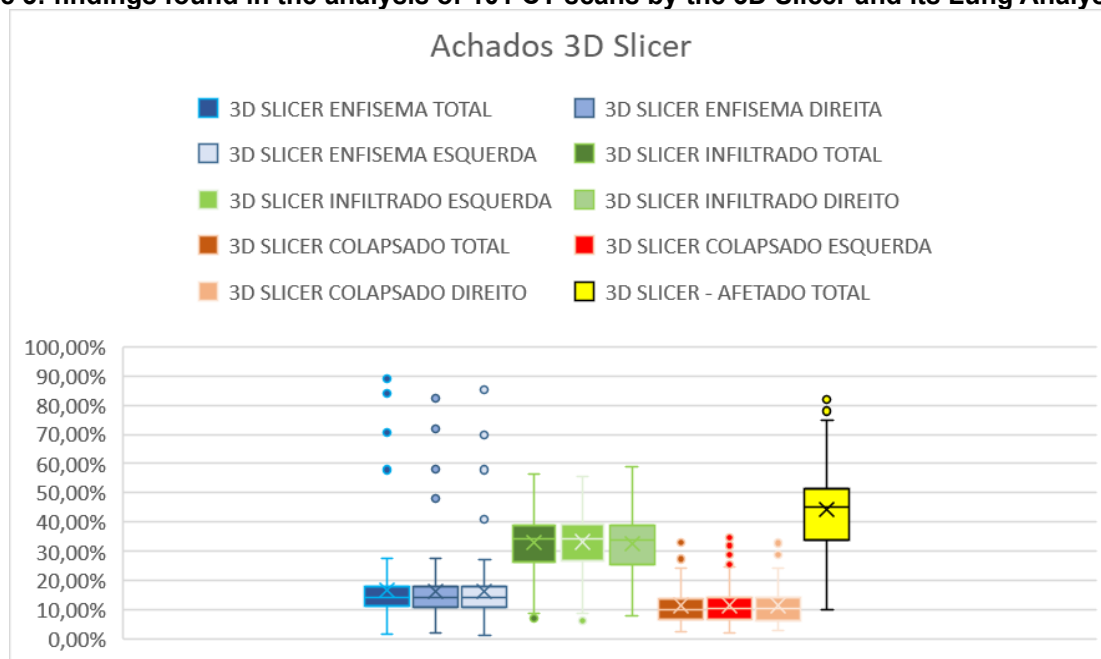
### Extended analysis (Table 2)

Lung area	Inflated + Affected (ml)	Inflated (ml)	Inflated (%)	Emphysema (ml)	Emphysema (%)	Infiltrated (ml)	Infiltrated (%)	Collapse (ml)	Collapse (%)	Affected (ml)	Affected (%)
Total lungs	1398	655	47	126	9	512	36.6	105	7.5	617	44
Right lung	909	499	55	73	8	342	37.6	68	7.5	410	45
Left lung	489	302	62	53	10.8	170	34.8	37	7.6	207	42

## 3 RESULTS

We analyzed 101 sets of images of patients with severe COVID-19 [defined as SpO<sub>2</sub> <94% on room air, ratio of partial pressure of oxygen to fraction of inspired oxygen (PaO<sub>2</sub>/FiO<sub>2</sub>) <300 mmHg, respiratory rate >30 breaths/min OR pulmonary infiltrates > 50%] or critical (individuals with respiratory failure, septic shock, and/or multi-organ dysfunction)(KENNETH MCINTOSH, 2022). The results described appear in Table 1, each row representing an image, and in Figure 3.

**Figure 3: findings found in the analysis of 101 CT scans by the 3D Slicer and its Lung Analyser tool**



The findings of emphysema remained around 20% of the lung volume (Figure 4 A), with a mean of 16.77% (SD=0.132), ranging from 1.6% to 89%. In pulmonary infiltrates, we have a mean of 32.98% involvement, with a standard deviation of 0.095, with results ranging from 7.1% to 56.4%. For the percentage of collapsed lungs, we have a mean of 11.48%, with involvement between 2.4 and 34.9% and a standard deviation of 0.067. The mean total percentage of lung affected was 44.3%, ranging from 10% to 82%, with a standard deviation of 0.15.

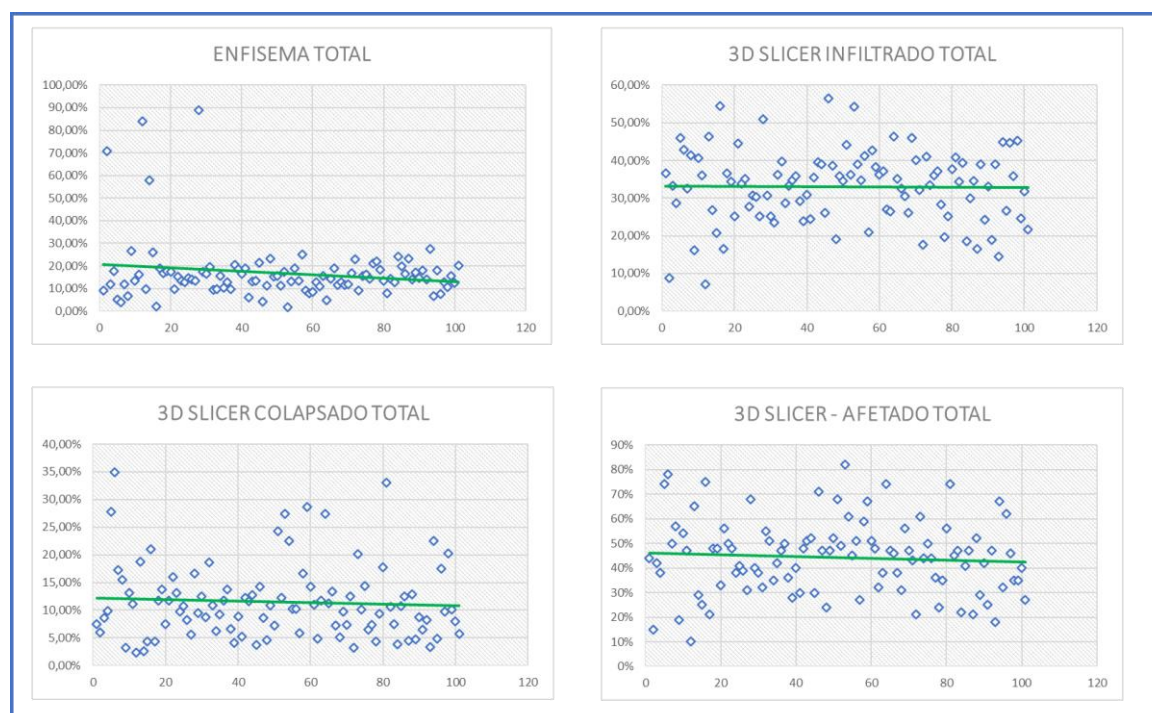
**Table 1: Overall result of the findings of each CT scan according to the 3D Slicer Software - Lung Analyser tool**

	3D TOTAL EMPHYSEMA SLICER	3D RIGHT EMPHYSEMA SLICER	3D LEFT EMPHYSEMA SLICER	3D TOTAL INFILTRATED SLICER	3D LEFT INFILTRATED SLICER	3D SLICER INFILTRATED RIGHT	3D TOTAL COLLAPSED SLICER	3D SLICER COLLAPSED LEFT	3D RIGHT COLLAPSED SLICER	3D SLICER R - TOTAL AFFECTED
1	9,00%	8,00%	10,80%	36,60%	34,80%	37,60%	7,50%	7,60%	7,50%	44%
2	70,70%	71,80%	69,70%	8,70%	8,80%	8,60%	6%	5,70%	6,30%	15%
3	11,90%	12,90%	10,80%	33,20%	34,10%	32,40%	8,60%	8,80%	8,40%	42%
4	17,80%	16,90%	18,80%	28,60%	27,50%	29,60%	9,90%	9,50%	10,30%	38%
5	5,00%	5,90%	4,10%	45,90%	49,10%	42,80%	27,80%	25,50%	30%	74%
6	3,90%	4,20%	3,60%	42,80%	42,90%	42,70%	34,90%	34,70%	35%	78%
7	12%	11,10%	13,10%	32,50%	30,30%	34,50%	17,30%	14,80%	19,70%	50%
8	6,80%	6,70%	6,90%	41,40%	37,20%	43,60%	15,50%	16,90%	14,80%	57%
9	26,50%	27,10%	25,80%	16,20%	15,60%	16,70%	3,20%	3,30%	3,10%	19%
10	13,30%	12,40%	14,30%	40,70%	39%	42,40%	13,10%	11,60%	14,50%	54%
11	16,30%	14,20%	18,50%	36,10%	33,60%	38,60%	11,10%	11,20%	10,90%	47%
12	83,90%	82,40%	85,30%	7,10%	6,20%	8,10%	2,40%	1,90%	3%	10%
13	9,70%	10,60%	8,60%	46,30%	47,70%	45,30%	18,80%	20,30%	17,60%	65%
14	57,90%	58,00%	57,90%	26,80%	26,90%	26,70%	2,60%	2,50%	2,80%	29%
15	25,90%	25,90%	26,00%	20,80%	21,10%	20,50%	4,40%	4,20%	4,50%	25%
16	2,10%	2,20%	2,00%	54,40%	55,40%	53,60%	21%	22,80%	19,70%	75%
17	18,90%	19,80%	17,90%	16,50%	17,60%	15,60%	4,40%	3,80%	4,90%	21%
18	16,80%	16,90%	16,70%	36,50%	39,20%	34,10%	11,70%	10,50%	13%	48%
19	17,70%	18,00%	17,40%	34,30%	34,70%	33,90%	13,70%	15,10%	12,40%	48%
20	17,30%	17,60%	17,00%	25,20%	27,20%	23,50%	7,50%	7,90%	7,10%	33%
21	9,60%	8,80%	10,40%	44,50%	41,30%	47,30%	11,80%	10%	13,40%	56%

22	15,20%	16,50%	14,30%	33,90%	36,10%	31,10%	16%	15,60%	16,50%	50%
23	13,50%	13,50%	13,60%	35,20%	37,90%	33,10%	13,10%	13,40%	12,80%	48%
24	12,90%	11,60%	14,20%	27,80%	25,80%	29,80%	9,80%	8,20%	11,30%	38%
25	14,60%	14,90%	14,20%	30,70%	31,30%	30,10%	10,70%	10,70%	10,70%	41%
26	14,00%	14,70%	12,90%	30,40%	33,60%	28,10%	8,20%	10,80%	6,40%	39%
27	13,40%	11,10%	15,60%	25,20%	22,20%	28,20%	5,60%	4,50%	6,70%	31%
28	89,00%	48,00%	41,00%	50,90%	52,30%	49,40%	16,70%	17,20%	16,20%	68%
29	17,30%	16,80%	17,90%	30,60%	29,90%	31,20%	9,50%	9,00%	9,90%	40%
30	16,50%	16,90%	16,10%	25,10%	25,80%	24,40%	12,50%	13,10%	12,00%	38%
31	19,50%	17,40%	21,60%	23,60%	21,60%	25,40%	8,80%	6,90%	10,60%	32%
32	9,50%	9,10%	10,00%	36,20%	36%	36,30%	18,70%	12,80%	23,70%	55%
33	9,60%	9,50%	9,60%	39,70%	38,70%	40,70%	10,90%	10,50%	11,20%	51%
34	15,50%	16,40%	14,20%	28,60%	32%	26,40%	6,30%	7,50%	5,40%	35%
35	10,30%	10,80%	9,50%	33,30%	37,20%	30,50%	9,20%	10,30%	8,40%	42%
36	12,70%	13,10%	12,30%	34,80%	37,20%	33,20%	11,80%	13,30%	10,70%	47%
37	9,80%	9,70%	9,90%	35,80%	35,90%	35,80%	13,80%	14,70%	13,20%	50%
38	20,50%	22,40%	18,30%	29,20%	33,50%	25,60%	6,60%	8,10%	5,40%	36%
39	18,70%	19,10%	18,10%	23,90%	25,50%	22,50%	4,10%	4,20%	4%	28%
40	16,40%	18%	14,40%	30,90%	33,40%	28,80%	8,90%	10,40%	7,80%	40%
41	18,80%	19,50%	17,90%	24,50%	25,20%	23,90%	5,20%	5,10%	5,40%	30%
42	5,90%	6%	5,70%	35,50%	36,60%	34,60%	12,30%	13,60%	11,20%	48%
43	13,20%	12,60%	13,80%	39,60%	38,40%	40,60%	11,60%	11,50%	11,70%	51%
44	13,50%	12,40%	14,20%	38,90%	38,60%	39,40%	12,70%	10,50%	16,30%	52%
45	21,50%	22,60%	20,10%	26%	28,20%	24,30%	3,70%	4%	3,40%	30%
46	4,20%	3,30%	5,30%	56,40%	53,30%	58,80%	14,20%	13,80%	14,50%	71%
47	11,20%	11,60%	10,80%	38,60%	38,40%	38,80%	8,60%	8,30%	8,90%	47%
48	23,30%	22,30%	24,50%	19,10%	18%	19,90%	4,60%	4,30%	4,80%	24%
49	15,20%	13,40%	17,10%	35,90%	32,30%	39,30%	10,90%	8,60%	13,20%	47%
50	15,70%	15,80%	15,70%	34,50%	34,30%	34,70%	7,30%	6,80%	7,80%	52%
51	11,30%	8,10%	15,90%	44,10%	40,40%	46,60%	24,30%	24,20%	24,30%	68%
52	17,40%	16,70%	18%	36,30%	36,30%	36,30%	12,30%	11,40%	13,10%	49%
53	1,60%	2,20%	1,20%	54,20%	53,70%	55%	27,40%	34,30%	17,40%	82%
54	13%	12,40%	13,50%	38,90%	39,30%	38,50%	22,50%	20,60%	24,40%	61%
55	18,80%	18,50%	19,10%	34,70%	33,60%	35,50%	10,20%	8,90%	11,20%	45%
56	13,50%	12,30%	14,80%	41,20%	39,40%	42,90%	10,20%	9,20%	11,20%	51%
57	25,10%	26,10%	24,10%	20,90%	23,10%	19,10%	5,90%	6%	5,90%	27%
58	9%	8,30%	9,70%	42,70%	41,60%	43,60%	16,60%	15%	18,10%	59%
59	8%	8,40%	7,50%	38,20%	39,20%	37,40%	28,70%	28,70%	28,70%	67%
60	8,60%	8,80%	8,30%	36,30%	35,80%	36,70%	14,30%	14,30%	14,30%	51%
61	12,90%	12,30%	13,60%	37,20%	36%	38,30%	11%	10,60%	11,30%	48%
62	11%	10,10%	12%	27,10%	26,40%	27,80%	4,90%	4,70%	5,10%	32%
63	15,60%	16%	15%	26,50%	28,80%	24,90%	11,70%	14,70%	9,60%	38%
64	4,70%	5,80%	3,40%	46,40%	50,80%	42,40%	27,40%	32%	23,30%	74%
65	14,30%	13,60%	15%	35,20%	36%	34,60%	11,30%	13,10%	9,80%	47%
66	19%	19,80%	17,90%	32,60%	34,70%	30,90%	13,40%	13,40%	13,40%	46%
67	11,60%	11,80%	11,40%	30,50%	33,30%	28,50%	7,30%	8,30%	6,30%	38%
68	12,90%	13,50%	12,20%	26,10%	26,90%	25,50%	5,10%	5,40%	4,80%	31%
69	11,50%	11,80%	11,20%	46%	46,40%	45,70%	9,80%	9,80%	9,80%	56%
70	11,80%	12,40%	11%	40%	41,70%	38,70%	7,40%	7,60%	7,20%	47%
71	16,90%	17,60%	15,90%	32,10%	29,80%	30,80%	12,50%	13,40%	12%	43%
72	23%	22,70%	23,50%	17,70%	17,10%	18,30%	3,20%	3%	3,40%	21%
73	9,20%	8,20%	10,20%	41%	41,60%	40,50%	20,20%	18%	22,50%	61%
74	15,50%	13,80%	17,40%	33,40%	31,70%	34,70%	10,10%	8,50%	11,50%	44%
75	16,20%	15,50%	16,80%	36%	35,50%	36,50%	14,40%	13,10%	15,80%	50%
76	14,20%	17,20%	10,40%	37,20%	45%	31,10%	6,50%	8,30%	5%	44%
77	21%	20,40%	21,60%	28,30%	24,60%	31,40%	7,40%	6,60%	8,10%	36%
78	22,10%	21,50%	22,80%	19,60%	19,50%	19,60%	4,30%	4,00%	4,50%	24%
79	18,20%	18,90%	17,10%	25,20%	27%	23,90%	9,40%	11,60%	7,90%	35%
80	13,40%	11,90%	15%	37,70%	35,20%	40,10%	17,80%	16,60%	19%	56%
81	8%	7%	9%	40,80%	39,00%	41,90%	33%	33,40%	32,80%	74%
82	14,30%	15%	13,60%	34,40%	35,30%	33,70%	10,60%	11,30%	9,90%	45%
83	12,80%	15%	10,30%	39,30%	43,90%	35,30%	7,50%	7,70%	7,30%	47%
84	24,10%	23,70%	24,50%	18,50%	18,40%	18,50%	3,90%	3,60%	4,20%	22%
85	20%	20,50%	18,80%	30%	32,20%	29%	10,80%	14,50%	9%	41%
86	16,60%	15,30%	18%	34,50%	32,50%	36,50%	12,50%	10,70%	14,20%	47%
87	23,20%	23%	23,40%	16,50%	16,70%	16,30%	4,50%	4,30%	4,60%	21%
88	14%	15,90%	11,30%	39%	42,50%	36,50%	12,90%	17,20%	10%	52%
89	17%	17,20%	16,50%	24,30%	25,50%	23,30%	4,70%	5,10%	4,30%	29%
90	14,60%	12,80%	16,50%	33%	30,40%	35,60%	8,80%	6,20%	11,20%	42%
91	18%	19,30%	16,30%	18,90%	22,10%	16,50%	6,50%	7,10%	6%	25%
92	13,90%	13,30%	14,30%	38,90%	42,90%	33,30%	8,30%	9,50%	6,70%	47%
93	27,40%	27,60%	27,30%	14,40%	15,40%	13,50%	3,30%	3,30%	3,30%	18%
94	6,70%	7,40%	6%	44,80%	46,10%	43,70%	22,50%	24,50%	20,70%	67%
95	17,90%	17,60%	18,20%	26,60%	28,50%	25,10%	4,90%	5,70%	4,40%	32%
96	7,70%	8,10%	7,30%	44,70%	43,80%	45,40%	17,50%	21,90%	21,90%	62%
97	12,90%	12%	14%	35,90%	36%	35,80%	9,70%	8,60%	10,70%	46%
98	10,70%	10,20%	11,10%	45,20%	45,80%	44,40%	20,30%	19,80%	20,80%	35%
99	15,40%	16,90%	13,90%	24,70%	27,90%	21,60%	10,10%	10,50%	9,80%	35%
100	12,40%	13,20%	11,60%	31,80%	32,70%	31%	8%	7,20%	8,80%	40%



**Figure 4 : (A) Total Emphysema, (B) Total infiltrate, (C) Total collapsed, and (D) Total affected.**



## 4 DISCUSSION

The Lung Analyser tool divides lung involvement into collapsed lung, emphysema, infiltrate, and inflated lung. Each of the lesions mentioned can influence the evolution of the disease, and consequently the outcome (HAN et al., 2023). Recognizing these lesions with greater sensitivity can contribute to patient decision-making and management. In our study, we observed that the vast majority of patients had a percentage of emphysema of around 20%, although some patients had very low levels of this type of lesion (1.6%), and others were very high, such as 89% (Figure 4A). When evaluating infiltrates, collapsed lungs, and the percentage of total involvement demonstrated by the Lung Analyser, this concentration was not observed around the same percentage, presenting an important plurality of results (Figures 4B, 4C, and 4D), despite a smaller variation among patients when compared to emphysema. Among the patterns analyzed, collapsed lung was the one with the lowest percentage. With the help of the description provided by semi-automatic or automatic tools such as the 3D Slicer, it is possible to improve the tomographic analysis, being able to help radiologists and, consequently, clinicians in defining the conducts to be taken.

The 3D Slicer Software is already used as a way to improve radiological accuracy in other organs and other types of diseases, such as neoplasms, including preoperative studies of spine surgeries in order to increase precision in screw implantation (WOOCHAN WI,SANG-MIN PARK, 2020),(X. HOU,D.-D. YANG, D. LI, L. ZENG, 2020),

(MURALIDHARAN et al., 2018). In the first study, the software helped surgeons handle accurate 3D information by simultaneously simulating surgery, and facilitating tumor location management for removal.

In a study published using 3 different software for the evaluation of the quantification of lung lesions by Covid-19, together with analysis by experienced radiologists, 3D Slicer demonstrated excellent reliability, with the best agreement between the software and the radiologist's analysis (RISOLI et al., 2022).

The processing of the images by the software is done in a few minutes, and the quantification of the percentage of pulmonary involvement and the appearance of the documented lesions can improve the description of the involvement in the radiological reports (RISOLI et al., 2022). Another important resource, shown in Figure 4, is that the report issued by the Lung Analyser classifies the percentage of pulmonary involvement pattern as infiltrate, emphysema, collapsed, and inflated lung, based on HU levels (HOCHHEGGER et al., 2010), information that is not always included in the CT scan report, mainly due to the way the reports are performed at the time. subjectively (MARTÍNEZ CHAMORRO et al., 2021), (SIMPSON et al., 2020), and can even be influenced by work overload at times such as a pandemic (CONEXÃO SAUDE, 2021).

Knowing in advance the type of lesion of the patient, differentiating, for example, a predominantly emphysematous pattern from a collapsed one, can also contribute to medical decision-making, considering the specificities of the management of patients' clinical conditions and their respective prognoses (PERONI; BONER, 2000), (CELIK et al., 2022). According to a study presented in 2020, the percentage of involvement is directly related to the risk of orotracheal intubation and death (LANZA et al., 2020). In addition, it is known that the evolution of the lesions is consistent with the moment of the disease (PÁDUA; WOULD; STRABELLI, 2020). Better recognition of these lesions, in a more reliable way, based on Artificial Intelligence (TSUNEKI, 2022), (SAN JOSÉ ESTÉPAR, 2022), can lead to better knowledge of the disease, influencing strategies for earlier treatments and better results.

## 5 CONCLUSION

The description of findings found by the 3D Slicer software and its Lung Analyser tool can be valuable for the identification and quantification of lung lesions in patients with COVID-19, reducing the subjectivity of the reports and helping to better understand lesions, which are sometimes not so visible to the human eye.

Being able to better identify the type of lung injury in patients, based on specific data such as the UH value and the possibility of more appropriate calculations in relation to its quantity, open opportunities for further studies and better identification of the lesions, as well as their progression, enabling the development of strategies and resources for the better management of these patients.

Although it is a tool in full development and with possibilities for evolution for better sensitivity in the detection of lesions, its use does not exclude the need for experienced radiologists for the best evaluation of such images, with the differentiation between the types of consolidation and especially when manual adjustments are necessary.

The Software has been shown to be able to identify lesions in an appropriate way, and with its frequent updating, it can be increasingly used for research, contributing to its release by regulatory agencies for clinical use.

## REFERENCES

1. 3D Slicer. (2023). Retrieved April 20, 2023, from <https://discourse.slicer.org/>
2. 3D Slicer COVID-19. (2020). New LungCTAnalyzer extension for lung CT segmentation and analysis for COVID-19 assessment. Retrieved December 21, 2021, from <https://discourse.slicer.org/t/new-lungctanalyzer-extension-for-lung-ct-segmentation-and-analysis-for-covid-19-assessment/15006>
3. 3D Slicer. (n.d.). About 3DSlicer. Retrieved December 25, 2022, from [https://slicer.readthedocs.io/en/latest/user\\_guide/about.html](https://slicer.readthedocs.io/en/latest/user_guide/about.html)
4. Bell, D., Murphy, A., Moreira, M., & et al. (n.d.). COVID-19. Radiopaedia.org. Retrieved March 14, 2023, from [https://radiopaedia.org/articles/covid-19-4#nav\\_radiology-report](https://radiopaedia.org/articles/covid-19-4#nav_radiology-report)
5. Celik, E., Nelles, C., Kottlors, J., Fervers, P., Goertz, L., Dos Santos, D. P., Achenbach, T., Maintz, D., & Persigehl, T. (2022). Quantitative determination of pulmonary emphysema in follow-up LD-CTs of patients with COVID-19 infection. PLoS ONE, 17(2), e0263261. <https://doi.org/10.1371/journal.pone.0263261>
6. Chang, Y. C., Yu, C. J., Chang, S. C., Galvin, J. R., Liu, H. M., Hsiao, C. H., Kuo, P. H., Chen, K. Y., Franks, T. J., Huang, K. M., & Yang, P. C. (2005). Pulmonary sequelae in convalescent patients after severe acute respiratory syndrome: Evaluation with thin-section CT. Radiology, 236(3), 1067–1075. <https://doi.org/10.1148/radiol.2363040958>
7. Colombi, D., Bodini, F. C., Petrini, M., Maffi, G., Morelli, N., Milanese, G., Silva, M., Sverzellati, N., & Michieletti, E. (2020). Well-aerated lung on admitting chest CT to predict adverse outcome in COVID-19 pneumonia. Radiology, 296(2), E86–E96. <https://doi.org/10.1148/radiol.2020201433>
8. Conexão Saúde. (2021). 32o Boletim - Conexão Saúde - Pandemia e colapso no sistema de saúde do Brasil. Retrieved from <http://pesquisa.bvsalud.org/bvsmis/resource/pt/mis-8122>
9. Han, K., Wang, J., Zou, Y., Zhang, Y., Zhou, L., & Yin, Y. (2023). Association between emphysema and other pulmonary computed tomography patterns in COVID-19 pneumonia. Journal of Medical Virology, 95(1), e28293. <https://doi.org/10.1002/jmv.28293>
10. Hani, C., Trieu, N. H., Saab, I., Dangeard, S., Bennani, S., Chassagnon, G., & Revel, M. P. (2020). COVID-19 pneumonia: A review of typical CT findings and differential diagnosis. Diagnostic and Interventional Imaging, 101(5), 263–268. <https://doi.org/10.1016/j.diii.2020.03.014>
11. Hochegger, B., Marchiori, E., Irion, K. L., & Oliveira, H. (2010). Accuracy of measurement of pulmonary emphysema with computed tomography: Relevant points. Radiologia Brasileira, 43(4), 260–265.
12. McIntosh, K. (2022). COVID-19: Clinical features. In UpToDate. Retrieved December 5, 2022, from [https://www.uptodate.com/contents/covid-19-clinical-features,righteous indignation-features?search=COVID-19&source=covid19\\_landing&usage\\_type=main\\_section#H4267089759](https://www.uptodate.com/contents/covid-19-clinical-features,righteous indignation-features?search=COVID-19&source=covid19_landing&usage_type=main_section#H4267089759)

13. Lanza, E., Muglia, R., Bolengo, I., Santonocito, O. G., Lisi, C., Angelotti, G., Morandini, P., Savevski, V., Politi, L. S., & Balzarini, L. (2020). Quantitative chest CT analysis in COVID-19 to predict the need for oxygenation support and intubation. *European Radiology*, 30(12), 6770–6778. <https://doi.org/10.1007/s00330-020-07013-2>
14. Martínez Chamorro, E., Díez Tascón, A., Ibáñez Sanz, L., Ossaba Vélez, S., & Borruel Nacenta, S. (2021). Radiologic diagnosis of patients with COVID-19. *Radiologia*, 63(1), 56–73. <https://doi.org/10.1016/j.rx.2020.11.001>
15. Menezes, M. C. S., Pestana, D. V. S., Gameiro, G. R., da Silva, L. F. F., Baron, É., Rouby, J. J., & Auler, J. O. C. (2021). SARS-CoV-2 pneumonia—receptor binding and lung immunopathology: A narrative review. *Critical Care*, 25(1), 1–13. <https://doi.org/10.1186/s13054-020-03399-z>
16. Muralidharan, V., Swaminathan, G., Devadhas, D., & Joseph, B. V. (2018). Patient-specific interactive software module for virtual preoperative planning and visualization of pedicle screw entry point and trajectories in spine surgery. *Neurology India*, 66(6), 1766–1770. <https://doi.org/10.4103/0028-3886.246281>
17. Oulefki, A., Agaian, S., Trongtirakul, T., & Kassah, A. (2020). Since January 2020 Elsevier has created a COVID-19 resource centre with free information in English and Mandarin on the novel coronavirus COVID-19. Elsevier Connect.
18. Pádua, L. de, & Farias, G. de, & Strabelli, D. G. (2020). Pneumonia por COVID-19 e o sinal do halo invertido. *Jornal Brasileiro de Pneumologia*, 46(2), e20200131.
19. Peroni, D. G., & Boner, A. L. (2000). Atelectasis: Mechanisms, diagnosis and management. *Paediatric Respiratory Reviews*, 1(3), 274–278. <https://doi.org/10.1054/prrv.2000.0059>
20. Prof. Rudolf Bumm, Department of Surgery, Kantonsspital Graubünden (KSGR). (n.d.). About LungAnalyser. Retrieved from <https://github.com/rbumm/SlicerLungCTAnalyzer>
21. Risoli, C., Nicolò, M., Colombi, D., Moia, M., Rapacioli, F., Anselmi, P., Michieletti, E., Ambrosini, R., Di Terlizzi, M., Grazioli, L., Colmo, C., Di Naro, A., Natale, M. P., Tombolesi, A., Adraman, A., Tuttolomondo, D., Costantino, C., Vetti, E., & Martini, C. (2022). Different lung parenchyma quantification using dissimilar segmentation software: A multi-center study for COVID-19 patients. *Diagnostics*, 12(6), 1501. <https://doi.org/10.3390/diagnostics12061501>
22. San José Estépar, R. (2022). Artificial intelligence in functional imaging of the lung. *British Journal of Radiology*, 95(1132), 20210527. <https://doi.org/10.1259/bjr.20210527>
23. Simpson, S., Kay, F. U., Abbara, S., Bhalla, S., Chung, J. H., Chung, M., Henry, T. S., Kanne, J. P., Kligerman, S., Ko, J. P., & Litt, H. (2020). Radiological Society of North America expert consensus document on reporting chest CT findings related to COVID-19: Endorsed by the Society of Thoracic Radiology, the American College of Radiology, and RSNA. *Radiology: Cardiothoracic Imaging*, 2(2), e200152. <https://doi.org/10.1148/ryct.2020200152>

24. Tsuneki, M. (2022). Deep learning models in medical image analysis. *Journal of Oral Biosciences*, 64(2), 159–165. <https://doi.org/10.1016/j.job.2022.03.003>
25. Wi, W., Park, S.-M., & Shin, B.-S. (2020). Computed tomography-based preoperative simulation system for pedicle screw fixation in spinal surgery. *Journal of Korean Medical Science*, 35(18), e125. <https://doi.org/10.3346/jkms.2020.35.e125>
26. Hou, X., Yang, D.-D., Li, D., Zeng, C. L. (2020). 3D Slicer and Sina application for surgical planning of giant invasive spinal schwannoma with scoliosis: A case report and literature review. *Neurochirurgie*, 66(5), 396–401. <https://doi.org/10.1016/j.neuchi.2020.06.129>
27. Xie, X., Zhong, Z., Zhao, W., Zheng, C., Wang, F., & Liu, J. (2020). Chest CT for typical 2019-nCoV pneumonia: Relationship to negative RT-PCR testing. *Journal of Clinical Microbiology*, 58(4), e00710-20. <https://doi.org/10.1016/j.jcv.2020.104384>
28. Zhou, S., Zhu, T., Wang, Y., & Xia, L. M. (2020). Imaging features and evolution on CT in 100 COVID-19 pneumonia patients in Wuhan, China. *European Radiology*, 30(10), 5446–5454. <https://doi.org/10.1007/s00330-020-06879-6>